Market Implications of Short-term Reserve Deliverability Enhancement

Fengyu Wang, Member, IEEE, Yonghong Chen, Senior Member, IEEE

Abstract — Midcontinent Independent System Operator (MI-SO) plans to introduce 30-minute short-term reserve (STR) to address 30 minutes system flexibility needs. Transmission bottlenecks in the power system may inhibit the deliverability of STR. Insufficient deliverable reserve may require additional operator manual adjustments, which may be uneconomic and distort the market price signal. To improve reserve deliverability, eventbased zonal STR clearing model and nodal STR clearing model are proposed to distribute reserve across the grid. This paper compares reserve deliverability and market clearing prices between the zonal STR model and the nodal STR model. A new design on penalty function is proposed in this paper to reflect the true value of security constraints for reserve deployment with the consideration of multiple events. Analysis of MISO test cases shows that the zonal approach is imprecise and may not guarantee the actual post-event flows within the physical limits. Nodal STR model can improve the reserve deliverability, market efficiency, and price signal.

Index Terms—Locational reserve payments, power generation dispatch, power system economics, reserve requirements, reserve zones, short-term reserve, unit commitment.

NOMENCLATURE:

I	Set of security constraints.
I^{REG}	Set of reserve deliverability constraints for regulation reserve.
I ^{CR}	Set of reserve deliverability constraints for contingency reserve.
I ^{STR}	Set of reserve deliverability constraints for short-term reserve.
J	Set of resources; $j, j \in J$.
K	Set of reserve zones; $k, k' \in K$
N	Nodes; $n(j) \in N$ is the node of resource j .
T	Periods $t \in T$.
X	Set of reserve categories {REG, SPIN, SUPP,

Fengyu Wang is with New Mexico State University, Las Cruces, NM 88003 USA. (email: fywang@nmsu.edu)

STR}. $x \in X$.

Disclaimer: The views expressed in this paper are solely those of the authors and do not necessarily represent those of MISO.

W Set of reserve deployment events {REGUP, REGDN, CR, STR}. $w \in W$.

 I^k Set of resources in zone k.

 \mathcal{E}^x Set of events for reserve x.

Parameters

 $B_{i,n,t}$ Sensitivity of the flow on transmission constraint i to injection at node n and withdrawal at the reference bus

 $B_{i,LC,t}$ Sensitivity of the flow on transmission constraint i to injection at market load center and withdrawal at the reference bus.

 $B_{i,k,t}^{x}$ Aggregated sensitivity of the flow on transmission constraint i to requirement for deployed reserve x in zone k and withdrawal at the reference bus

 $B_{i,k,t}^{TRIP}$ Aggregated sensitivity of the flow on transmission constraint i to the largest contingency event in zone k with injections at the locations used to model the outage and withdrawal at the reference bus.

 $C_{i,t}^P$ Energy production cost of resource j, in \$/MWh

 $D_{k,t}^{SPIN}$ Spinning reserve deployment factor under the largest contingency event in zone k.

 $D_{k,t}^{SUPP}$ Supplemental reserve deployment factor under the largest contingency event in zone k.

 $E_{e,t}^{x}$ Event *e* for reserve *x*.

 $R_{MKT.t}^{x}$ System-wide requirement for reserve x.

 $\overline{F}_{i,t}$ Flow limit on constraint i

 $O_{j,t}^{x}$ Resource j available offer price for reserve x, in MWh

 $P_{n,t}$ Net fixed injection at node n

 L_t Interval length of interval t, in minutes

 $\bar{P}_{i,t}$ Resource j maximum power output.

 $\underline{P}_{i,t}$ Resource j minimum power output.

 $U_{i,t}$ Commitment status for resource j

 $V_{i,t}^{UP}$ Resource j up ramp rate in MW/min

 $V_{i,t}^{DOWN}$ Resource j down ramp rate in MW/min

Yonghong Chen is with Midcontinent Independent System Operator (MI-SO), Carmel, IN 46032 USA (e-mail: ychen@misoenergy.org).

Variables (index t denotes period):

onstraint <i>i</i>

 $p_{j,t}$ Cleared energy on resource j

 $r_{i,t}^x$ Cleared reserve x on resource j

 $y_{k,t}^x$ Cleared zonal reserve x on zone k

 $h_{n,t}^{STR}$ Cleared STR on node n.

 $q_{k,e,t}^{STR}$ Deployed zonal STR on zone k for event e

 $g_{n\,e\,t}^{STR}$ Deployed STR on node n for event e

Market Clearing Prices:

 $MCP_{k,t}^{x}$ Zonal MCP for reserve x zone k

 $LMP_{n,t}^{ZSTR}$ Locational marginal price of zonal model for node n

 $LMP_{n,t}^{NSTR}$ Locational marginal price of nodal model for node n

I. INTRODUCTION

INCERTAINTIES from load, renewables, area interchange, and contingencies introduce challenges in managing system reliability and efficiency. To ensure continuous service to the load, ancillary services such as operating reserves are employed to provide backup capacitiy. Independent system operators (ISOs) co-optimize energy and ancillary service to maximize market surplus under constraints such as power balance and transmission limits while considering resource costs and physical constraints. For instance, securityconstrained unit commitment (SCUC) and securityconstrained economic dispatch (SCED) are used to clear the day-ahead and real-time market with co-optimization of energy and ancillary services at Midcontinent Independent System Operator (MISO). Many studies have been performed in cooptimizing energy and ancillary service [1]-[3]. Based on the response time and functionality, operating reserve can be categorized into three types [4] in MISO: regulation, spinning reserve, and supplemental reserve. Regulation reserve adjusts its generation output based on the feedback of area control error through central automatic generation control and it can be used to follow small system variations within several seconds. Spinning reserve and supplemental reserve, which are supposed to respond within 10 minutes, are used to protect against large system perturbations such as contingencies.

Some of the operational constraints are required to be addressed within 30 minutes. Examples of 30 minutes system operating requirements in the MISO system are post-contingency event restoration of 1) regional dispatch transfer (RDT) limits between MISO north/central and south regions 2) System Operating Limit (SOL) constraints. Any violation on RDT or SOL under a large contingency event should be addressed within 30 minutes. It is uneconomic to address these 30 minutes issues with a high premium 10-min operating reserve. Furthermore, MISO has some load pockets with limited importing capability and insufficient quick-start units. Without a 30-min product, operators need to manually commit re-

sources in the load pockets to meet reliability requirements on operation on RDT and SOL constraints. Therefore, MISO plans to introduce a 30-minute short-term reserve (STR) and co-optimize it with energy and other ancillary services in both the day-ahead market and real-time market. STR, which can provide energy within a relatively short period (e.g. 30 minutes), is an important tool for maintaining reliability. It can provide the ability to manage capacity needs that may not be addressed by operating reserves. Including STR in the market design will 1) improve commitment process related to load pockets due to RDT and SOL constraints; 2) improve the transparency of cost associated with 30 minutes system needs in managing uncertain events; 3) enhance system reliability by aligning operational needs and market clearing processes; 4) improve flexibility to meet load and supply volatility and variability under future portfolio changes. Existing market products do not produce enough price signals to incentivize generating resources provide products and new investment that addresses load pocket issues. Introducing STR in the market could improve the commitment progress by reducing out of market commitments and produce additional market price signals on load pockets issues on top of existing market prod-

Similar to operating reserves, STR may be not dispatchable due to network congestion under contingency scenarios. The dispatchability of STR under network congestion is referred to as reserve deliverability. Insufficient deliverable reserves may requires out of market corrections (OMCs) to ensure system reliability. CAISO refers to such OMCs as uneconomic adjustments or exceptional dispatches [5]-[6], and exceptional dispatches are used to obtain feasible dispatch solutions when economic dispatch optimization engine cannot guarantee reliability. Electric Reliability Council of Texas (ERCOT) refers to OMCs as out of merit capacity to ensure sufficient generating capacity. Such out of market corrections will incur additional operating costs [7]-[8]. MISO utilizes manual dispatch to adjust the dispatch solution to obtain a reliable solution [9]. To alleviate potential risk to system reliability, MISO operators may manually disqualify undeliverable reserves. Such an ad-hoc manual correction procedure is outside the energy and ancillary service co-optimization process and in some circumstances, operators may disqualify a large number of reserves to guarantee a sufficient amount of deliverable reserve, which may incur significant cost. Furthermore, implementing reserve disqualifications under a deregulated market structure will also distort market clearing prices.

To improve reserve deliverability, some ISOs utilize a zonal approach to distribute the reserve across their system. In [2], the Independent System Operator of New England (ISO-NE) allows reserve shared from child reserve zone to parent reserve zone with the consideration of transmission bottlenecks. However, the congestion patterns are difficult to predict. MI-SO started with pre-defined market-wide and zonal reserve requirements. Due to the forecasting error and variability of the power system, the scenarios studied two days prior to the operating day could be quite different from the actual operating conditions, and thus, the allocated reserve by pre-defined zonal reserve requirements may not be deliverable, and operators may manually disqualify undeliverable reserve to ensure reliability.

One way to improve reserve deliverability is by improving reserve zones. In [10] and [11], Wang et al. developed a dynamic reserve zone determination approach based on statistical clustering method with consideration of system sensitivities, and this reserve zone determination method updates the reserve zones on a daily basis while considering the system operating condition. It is shown that updating the reserve zone definition on a more frequent basis will lower the violations and improve the market efficiency and system reliability. In [12], the market aspects of an hourly reserve zone determination method are evaluated. The quality of ancillary service is improved by the proposed hourly reserve zone determination method. However, re-configuring reserve zone on an hourly basis requires significant change to the market clearing engine. Furthermore, reserve zone is still an approximation of allocating reserve across the grid. In [13], Chen et al. enhance the co-optimization model to improve the reserve deliverability by incorporating post zonal reserve deployment transmission constraints for the largest contingency in each reserve zone. Zonal reserve deployment transmission constraints model the post event power flow on the pre-selected transmission constraints with the consideration of deployed reserves under the events. Reserves are deployed on a zonal level and the zonal reserve requirements are optimally allocated through the clearing process. The formulation proposed in [13] has been implemented in MISO since 2013 and it has improved the operating reserve deliverability for critical transmission interface constraints across zones. One assumption of the zonal approach is that nodes inside the same reserve zone will have the same zonal sensitivity, which is the aggregated value of nodal sensitivities. Zonal sensitivities are used to approximate the reserve deployment's impact on transmission assets. The system operating condition changes all the time, but the reserve zone definition of MISO is reconfigured on a quarterly basis. Usually little or no change is made in the reserve zone re-configuration process. Therefore, the post zonal reserve deployment approach cannot fully solve the issue of the undeliverable reserve due to the inaccuracy of zonal approximation of sensitivities and it cannot guarantee reserve deliverability. PJM proposes a closed loop reserve sub-zone to further refine the existing reserve zone [14]. The sub-zone concept aims to improve reserve deliverability and market pricing signals.

In [15], an adjustable robust optimization model procures energy and reserve with the consideration of spatially correlated nodal demand and N-1 contingencies. Adjustable robust optimization can protect against the worst-case pre-defined uncertainty set by clearing reserve from explicit generating resources. The reserve costs are significantly impacted by the conservativeness parameters and robust unit commitments are not computationally scalable. In [16], a robust optimization framework is used to established to address the deliverability flexible ramping products and Deliverable Robust Ramping Product is derived to reflect the cost of deliverability. In [17], an AC-OPF based two-step market clearing is proposed to clear energy and contingency reserves with the consideration of customers' nodal unit commitment risk. AC-OPF is not adopted by industry due to convergence issues. A locational pricing scheme is developed based on Lagrange multipliers in [18]. Pricing interactions among different types of reserve are not considered in [18] and different deployment logics of reserve have significant impacts on pricing solutions.

Stochastic programming can be used to implicitly determine the reserve by modeling a set of uncertainty scenarios [19]-[23]. To better locate the reserve, Bouffard et al. [21] proposed to co-optimize energy and reserve with consideration of both pre-contingency and post-contingency power balance and transmission constraints. The proposed formulation in [22] explicitly determines the quantity and location of reserve, but the increased computational complexity of the added problem size limits the use of this proposed stochastic extensive formulation. It is even computationally challenging to solve deterministic SCUC in the MISO system [24]-[25]. Scenario reduction technique [26]-[27] can be used to select a subset of scenarios modeled to reduce the computational burden. However, it is difficult to find a subset of scenarios to protect against the complete set of uncertainty scenarios. Furthermore, stochastic programming also requires a complete market design overhaul and better pricing interpretations of stochastic scenarios. Therefore, there is a need to improve reserve deliverability through market clearing price signals and reduce OMCs while maintaining existing deterministic framework.

The contributions of this paper are as follows,

- Zonal STR model and nodal STR model are proposed to address system 30 minutes flexibility needs. Zonal and nodal formulations are compared with regards to deliverability.
- 2) The market impacts of zonal and nodal STR models are extensively studied. Nodal model tends to provide a more efficient STR price signal than the zonal model. The interaction between the prices of STR and other market products (e.g., locational marginal prices (LMPs) and operating reserve market clearing prices (MCPs) is also investigated.
- 3) This paper proposes an innovative penalty function design to avoid exaggerating the value of a security constraint under multiple binding post-event security constraints in comparison to the existing design [13].

The remainder of this paper is organized as follows. Section II discusses zonal and nodal STR requirement design, associated market implications, and penalty function design. Numerical results are shown in Section III. Section IV concludes this paper.

II. SHORT-TERM RESERVE REQUIREMENTS DESIGN

MISO co-optimizes energy and ancillary service every 5 minutes in the real-time security constrained economic dispatch (RT-SCED) market clearing software. RT-SCED collects system information with 10 minutes load and renewable forecasts as inputs. It solved a single interval SCED at time t and its solutions set the energy target for generating resources at t+10 minutes. However, existing single interval RT-SCED does not consider 30-minutes system flexibility needs, which may require pre-ramping, holding ramping capability, or redispatching. The proposed STR aims to achieve more economic market solutions in real-time without modeling multiple intervals under post contingency events, which requires complicated stochastic optimization. 30-min reserve requirement is driven by the regional reliability requirement of restor-

ing regional transfer limit within 30-min after the contingency event. In some regions, there are not always enough 30-min online or offline resources to guarantee 30-min restoration. Historically operations need to address the issue through outof-market actions. Hence, introducing 30-min STR is important for maintaining reliable operation and producing system wide and/or regional investment signals.

Similar to operating reserves, it's important to clear STR at the right location to guarantee deliverability when deployed. Two STR models are proposed and compared in this section. The existing SCED formulation in MISO is listed in Appendix A in equations (30)-(46).

A. Zonal and Nodal STR Models

In this section, zonal and nodal STR formulations, as presented in Table I, will be discussed and compared.

Constraints (1a) and (1b) define system-wide STR requirement, which quantifies system-wide short-term reserve needs. Zonal model requires the summation of cleared zonal STR reserve $y_{k,t}^{STR}$ no less than the system-wide STR requirement. Nodal model requires the summation of cleared nodal STR reserve $h_{n,t}^{STR}$ no less than the system-wide STR requirement. Constraints (2a) and (2b) bound the maximum STR deployment by cleared STR on zonal and nodal basis, respectively. The zonal model defines dynamic zonal reserve requirement $y_{k,t}^{STR}$ shown in constraint (3a) while the nodal model defines dynamic nodal reserve requirement $h_{n,t}^{STR}$, in constraint (3b). The nodal requirement is more accurate in reflecting specific locational needs. The dynamic reserve requirements $y_{k,t}^{STR}$ and $h_{n,t}^{STR}$ are variables and they are internally balanced by STR post-event power balance constraints (4a,b) and STR post-event deliverability constraints (5a,b) so the loca-

tional STR requirement is optimized. The zonal model employs zonal aggregated sensitivities $B_{i,k,t}^{STR}$ while the nodal model directly uses nodal sensitivities $B_{i,n,t}$ to capture STR deployment and the event's impacts on the constraint flow. Zonal model assumes nodes in the same zone have the same zonal sensitivities. However, nodes in the same zone may have quite different nodal sensitivities on some transmission lines, especially for transmission constraints within a zone. Constraint (6) indicates that STR share capacity with spinning and supplemental reserves but not regulation reserve. The reason is that spinning and supplemental reserves deployed in the first 10 minutes can be counted towards 30 minutes STR deployment, all on the upwards direction. Regulation reserve cleared at MISO can be deployed up or down. Note that the symbol following each type of constraint represents corresponding shadow prices.

Unlike operating reserves, which have pre-determined deployment factors, STR relies on economic dispatch in realtime within 30 minutes of the contingency event. Therefore, the post-event power balance constraint is needed to guarantee that deployed STRs exactly meet the size of the event. Postevent deliverability constraints model constraint flow considering the impacts of the event and STR deployment. It's applied to RDT and SOL transmission constraints to ensure post deployment flows on these constraints are restored to their limits within 30-min. Reserve zones are pre-defined based on the same set of IROL, RDT, and SOL transmission constraints. Note that both zonal and nodal STR models maintain a deterministic framework by pre-determining the largest zonal events. The increased computational burden of the eventbased post reserve deployment constraints is minimal.

Table I Zonal and Nodal STR Formulations					
STR Constraints	Zonal Model		Nodal Model		
System-wide STR requirement	$\sum_{k \in K} y_{k,t}^{STR} \ge R_{MKT,t}^{STR} \left\{ \gamma_t^{MSTR} \right\}$	(1a)	$\sum_{n \in N} h_{n,t}^{STR} \ge R_{MKT,t}^{STR} \left\{ \gamma_t^{MSTR} \right\}$	(1b)	
Maximum STR de- ployment	$q_{k,e,t}^{STR} \le y_{k,t}^{STR} \left\{ \varphi_{k,e,t}^{ZSTR} \right\}$	(2a)	$g_{n,e,t}^{STR} \leq h_{n,t}^{STR} \left\{ arphi_{k,e,t}^{NSTR} ight\}$	(2b)	
Locational STR requirement	$\sum_{j \in J^k} r_{j,t}^{STR} \ge y_{k,t}^{STR} \left\{ \tau_{k,t}^{ZSTR} \right\}$	(3a)	$\sum_{j \in I^n} r_{j,t}^{STR} \ge h_{n,t}^{STR} \left\{ \tau_{n,t}^{NSTR} \right\}$	(3b)	
STR post-event power balance constraint	$\sum_{k \in K} q_{k,e,t}^{STR} = E_{e,t}^{STR} \left\{ \sigma_{e,t}^{ZSTR} \right\}$	(4a)	$\sum_{n \in N} g_{n,e,t}^{STR} = E_{e,t}^{STR} \left\{ \sigma_{e,t}^{NSTR} \right\}$	(4b)	
STR post-event deliv- erability constraint	$f_{i,t} - E_{e,t}^{STR} B_{i,e,t}^{TRIP} + \sum_{k \in K} (q_{k,e,t}^{STR} B_{i,k,t}^{STR}) \le \overline{F}_{i,t} \{ \mu_{i,e,t}^{ZSTR} \}$	(5a)	$f_{i,t} - E_{e,t}^{STR} B_{i,e,t}^{TRIP} + \sum_{k \in K} \left(g_{n,e,t}^{STR} B_{i,n,t} \right) \le \overline{F}_{i,t} \left\{ \mu_{i,e,t}^{NSTR} \right\}$	(5b)	
Resource capacity constraints	$p_{j,t} + r_{j,t}^{REG} + r_{j,t}^{STR} \le U_{j,t} \overline{P}_{j,t} $ (6)				

Table II Market Prices of Zonal and Nodal STR Models Market Prices Zonal Model Nodal Model Regulation Reserve $MCP_{k,t}^{SPIN} = \gamma_{kt}^{ZRS} + \gamma_{kt}^{ZOR}$ (8) Spinning Reserve Supplemental Reserve Short-term Reserve Locational Marginal Prices

B. Market Implications of STR Design

This section will discuss the market impacts of proposed STR models on reserves and energy and how the market prices of different products interact with each other. Wholesale electricity markets in the United States follow the concept of marginal pricing [28], the operating reserve market clearing prices (MCP) are listed in equations (7)-(9) from Table II. Zonal and Nodal STR models do not impact the pricing structure of operating reserves.

Post-event deliverability constraints of operating reserve and STR include the power flow variable $f_{i,t}$, Hence, LMPs of zonal and nodal STR model has four congestion components from security constraints of energy, post-event deployment security constraints of regulation reserve, contingency reserve, and short-term reserve as shown in equations (11a) and (11b) from Table II. The proof of the Karush-Kuhn-Tucker (KKT) condition for LMPs (11a) and (11b) can be found in Appendix B. These components indicate the marginal cost of relieving corresponding constraints with 1MW injection or withdraw at each node. If an STR post-event deliverability constraint is will be impacted binding, **LMPs** $\sum_{i \in ISTR} \sum_{e \in \mathcal{E}STR} \mu_{i,e,t}^{ZSTR} B_{i,n,t} \quad \text{or} \quad \sum_{i \in ISTR} \sum_{e \in \mathcal{E}STR} \mu_{i,e,t}^{NSTR} B_{i,n,t} \; .$ The STR congestion component reflects the opportunity cost of preserving the transmission capacity for post-event security. Furthermore, energy will interact with reserve clearings by trading off between pre-contingency flow and locational procurement of reserves. If deliverable reserves are costly or unavailable, the market clearing engine may re-dispatch generation to lower the pre-contingency flow such that the system is secure post-event. Therefore, scarcity in deliverable reserves may result in higher energy congestion components, which may result in higher LMPs.

Based on the concept of marginal pricing, the market clearing prices of STR can be obtained from equations (10a) and (10b) for zonal and nodal STR models respectively.

Based on the duality theory, the dual constraints for primal variables $q_{k,e,t}^{STR}$ and $y_{k,t}^{STR}$ from zonal STR model are $\varphi_{k,e,t}^{ZSTR} + \sigma_{e,t}^{ZSTR} + \sum_{i \in ISTR} \mu_{i,e,t}^{STR} B_{i,k,t}^{STR} = 0$

$$\varphi_{k,e,t}^{ZSTR} + \sigma_{e,t}^{ZSTR} + \sum_{i \in I} STR \mu_{i,e,t}^{STR} B_{i,k,t}^{STR} = 0$$
 (12)

$$\gamma_t^{MSTR} - \sum_{e \in \mathcal{E}^{STR}} \varphi_{k,e,t}^{ZSTR} - \gamma_{k,t}^{ZSTR} = 0$$
 (13)

From equations (12) and (13), STR price of zonal model is

$$\gamma_{k,t}^{ZSTR} = \gamma_t^{MSTR} + \sum_{e \in E} \sigma_{e,t}^{ZSTR} + \sum_{i \in ISTR} \sum_{e \in \mathcal{E}^{STR}} \mu_{i,e,t}^{ZSTR} B_{i,k,t}^{STR} (14)$$

Similarly, the dual constraints for primal variables $g_{n,e,t}^{STR}$ and $h_{n,t}^{STR}$ from the nodal model are: $\varphi_{k,e,t}^{NSTR} + \sigma_{e,t}^{NSTR} + \sum_{i \in ISTR} \mu_{i,e,t}^{STR} B_{i,n,t} = 0$

$$\varphi_{k,e,t}^{NSTR} + \sigma_{e,t}^{NSTR} + \sum_{i \in I} STR \, \mu_{i,e,t}^{STR} B_{i,n,t} = 0 \tag{15}$$

$$\gamma_t^{MSTR} - \sum_{e \in \mathcal{E}STR} \varphi_{k,e,t}^{NSTR} - \tau_{n,t}^{STR} = 0 \tag{16}$$

From equations (15) and (16), STR price of nodal model is

$$\tau_{n,t}^{STR} = \gamma_t^{MSTR} + \sum_{e \in E} \sigma_{e,t}^{NSTR} + \sum_{i \in ISTR} \sum_{e \in \mathcal{E}STR} \mu_{i,e,t}^{NSTR} B_{i,n,t}(17)$$

Based on equations (14) and (17), both zonal STR price $\gamma_{k,t}^{ZSTR}$ and nodal STR price $\tau_{n,t}^{STR}$ has three components i) system-wide STR requirement component γ_t^{MSTR} , ii) STR postevent zonal power balance component, $\sum_{e \in E} \sigma_{e,t}^{ZSTR} / \sum_{e \in E} \sigma_{e,t}^{NSTR}$, iii) STR post-event reserve deliverability constraint component, $\sum_{i \in ISTR} \sum_{e \in ESTR} \mu_{i,e,t}^{ZSTR} B_{i,k,t}^{STR}$ $\sum_{i \in I} STR \sum_{e \in \mathcal{E}} STR \mu_{i,e,t}^{NSTR} B_{i,n,t}.$

Similar to LMP, the congestion component of STR price indicates the deliverability of cleared reserve. STR in deliverable locations tend to receive positive congestion components while STR in stranded locations tend to receive negative congestion components. Constraint (3b) defines the STR requirement on a nodal basis. This design can avoid resource-based pricing and negative prices of STR, which stochastic SCED may have in market design issues. Unlike zonal STR model, nodal STR model distinguishes STR deliverability on a nodal basis by employing nodal sensitivity $B_{i,n,t}$ instead of $B_{i,k,t}^{STR}$. Such nodal STR requirement will lead to nodal STR prices. Nodal STR price is supposed to provide a better price signal than the zonal model. STR cleared by the zonal model may still receive high prices even though it is not fully deliverable on a nodal basis. The congestion component $\mu_{i,e,t}^{NSTR}B_{i,n,t}$ of STR price from the nodal model is also consistent with STR congestion component in LMP $\mu_{i,e,t}^{NSTR}B_{i,n,t}$. Zonal STR receive zonal congestion component $\mu_{i,e,t}^{ZSTR}B_{i,k,t}^{STR}$ while LMP of zonal model still receives nodal STR component $\mu_{i,e,t}^{ZSTR}B_{i,n,t}$. Therefore, the nodal STR model is more consistent in price signals.

Regulation reserve, spinning reserve, and supplemental reserve have cascading pricing structure as demonstrated in equations (7)-(9). Equations (7)-(9) allow scarcity pricing of spinning/supplemental reserves reflected in the regulation prices. Unlike cascading structures of operating reserves, constraint (6) allows that the same generation capacity can be cleared as spinning/supplemental reserve and STR at the same time. Constraint (6) can still award capacity at the same time if the capacity is cleared for both spinning/supplemental reserves and STR. However, operating reserves prices do not necessarily receive the scarcity pricing of STR if STR capacity is scarce.

C. Penalty Function Design for Post-Event Constraints

In most ISOs/RTOs market design, ancillary service constraints and security constraints are modeled as soft constraints, which will cap the associated shadow prices [29]. The soft constraint can reflect the fact that not all operational procedures are included in the market clearing model. For example, most violations on transmission constraints are allowed to be restored in multiple dispatch intervals. There are also multi-step emergency procedures to commit or dispatch emergency capacities including load curtailment. To balance economic efficiency and system reliability, the reserve demand curve could value reserves by different levels of reserve requirements instead of flat and fixed reserve requirements. However, it is challenging to design the demand curve with the consideration of post-event constraints, especially the reserve deliverability.

The transmission constraint demand curve (TCDC) is used by the RTOs to restrict the cost of managing a constraint through energy re-dispatching [30]. One transmission element should at most correspond to one post contingency security constraints with TCDC since the RTO is only required to be N-1 secure. Otherwise, the transmission element may be overvalued when the TCDC is be stacked for different post contingency security constraints corresponding to the same transmission element. However, for STR, one transmission element can correspond to multiple STR post-event deployment constraints. To avoid infeasibility, slack variables are also needed for STR post-event power balance constraints. The functions of post-event constraints can be formulated for zonal and nodal models as below by introducing slack variables to each constraint.

1) STR post-event deliverability constraint ($\mu_{i,e,t}^{STR}$)

$$f_{i,t} - E_{e,t}^{STR} B_{i,e,t}^{TRIP} + \sum_{k \in K} (q_{k,e,t}^{STR} B_{i,k,t}^{STR}) \le \overline{F}_{i,t} + s_{i,e,t}^{PED}$$
(Zonal) (18)

$$f_{i,t} - E_{e,t}^{STR} B_{i,e,t}^{TRIP} + \sum_{k \in K} (g_{n,e,t}^{STR} B_{i,n,t}) \le \overline{F}_{i,t} + s_{i,e,t}^{PED}$$
(Nodal) (19)

2) STR post-event power balance constraint ($\sigma_{e,t}^{STR}$)

$$\sum_{k \in K} q_{k,e,t}^{STR} = E_{e,t}^{STR} + s_{e,t}^{PB+} - s_{e,t}^{PB-}$$
(Zonal) (20)

$$\sum_{n \in N} g_{n,e,t}^{STR} = E_{e,t}^{STR} + s_{e,t}^{PB+} - s_{e,t}^{PB-}$$
(Nodal) (21)

The reserve requirements are event-based the demand curve and associated slack variables must be designed accordingly to reflect the true value of associated reserve requirements and avoid overpricing. The penalty function design for post-event constraints can significantly impact the value of STR products. Two different ways of modeling the penalty cost of STR products in the objective $\min_{p_{j,t},r_{j,t}^x} \sum_{j \in J} \{C_{j,t}^P p_{j,t} + C_{j,t}^P p_{j,t}\}$

$$\sum_{x \in X} (O_{j,t}^x r_{j,t}^x) + s_t^{STR}$$
 are presented as follows: Option 1: (κ_t^{STR})

$$s_t^{STR} = \sum_{i} \sum_{e} \Psi_{i,e,t}^{PED} s_{i,e,t}^{PED} + \sum_{e} \Psi_t^{PB} (s_{e,t}^{PB+} + s_{e,t}^{PB-})$$
 (22)

Option 2: $(\kappa_{e.t}^{STR})$

$$s_{t}^{STR} \geq \sum_{i} \Psi_{i,e,t}^{PED} \, s_{i,e,t}^{PED} + \Psi_{t}^{PB} \left(s_{e,t}^{PB+} + s_{e,t}^{PB-} \right) \ \ \, \forall e \in \mathcal{E}^{STR} \ \ \, (23)$$

 Ψ^{PB}_t is the demand curve price for post-event power balance constraint, $\Psi^{PED}_{i,e,t}$ is the demand curve price for post-event deliverability constraints. For simplicity, it is assumed that the demand curve in this paper is a single step, but the conclusions are easy to expand to multi-step demand curves. Option 1 summates the penalty cost over all the events, which was used in [13], while option 2 only considers the event that incurs the highest penalty cost. Option 1 and option 2 could result in significantly different STR prices and LMPs. Table III presents slack variables and associated dual constraints.

Table III Slack Variable and associated dual constraints

Primal	Dual Constraints			
Variables	Option 1 [13]	Option 2		
$S_{i,e,t}^{PED}$	$\mu_{i,e,t}^{STR} - \Psi_{i,t}^{PED} \kappa_t^{STR} \le 0 \tag{24a}$	$\mu_{i,e,t}^{STR} - \Psi_{i,t}^{PED} \kappa_{e,t}^{STR} \le 0 \text{ (24b)}$		
$S_{e,t}^{PB+}$, $S_{e,t}^{PB-}$	$\left \sigma_{e,t}^{STR}\right - \Psi_t^{PB} \kappa_t^{STR} \le 0 \text{ (25a)}$	$\left \sigma_{e,t}^{STR}\right - \Psi_t^{PB} \kappa_{e,t}^{STR} \le 0 \text{ (25b)}$		
S_t^{STR}	$\kappa_t^{STR} = 1 (26a)$	$\sum_{c} \kappa_{e,t}^{STR} = I(26b)$		

Based on (24a), (25a), and (26a),

$$\mu_{i,e,t}^{STR} \le \Psi_{i,t}^{PED} \text{ and } \left| \sigma_{e,t}^{STR} \right| \le \Psi_{t}^{PB}$$
 (27)

Based (24b), (25b), and (26b),

$$\sum_{e} \mu_{i,e,t}^{STR} \le \Psi_{i,t}^{PED} \sum_{e} \kappa_{e,t}^{STR} = \Psi_{i,t}^{PED}$$
(28)

$$\sum_{e} \left| \sigma_{e,t}^{STR} \right| \le \sum_{e} \Psi_{t}^{PB} \kappa_{e,t}^{STR} = \Psi_{t}^{PB} \sum_{e} \kappa_{e,t}^{STR} = \Psi_{t}^{PB}$$
 (29)

North American Electric Reliability Corporation requires system operators to maintain N-1 reliability criteria, which assumes a loss of transmission asset or generator asset at a time. Therefore, shadow prices of event-based deliverability constraints should not accumulate if multiple deliverability constraints on the same transmission asset bind for different events at the same time. We propose the penalty function to reflect the worst violation among all the events. Otherwise, the STR congestion component on the associated transmission asset will be overvalued. The shadow prices on the same transmission element will be stacked and the optimization engine may re-dispatch expensive units to mitigate STR deliverability constraints. Inequality (27) shows that under option 1, each STR constraint may reach the associated demand curve prices. When post deployment constraints are violated under multiple events for the same security constraint i, the penalty price may be multiplied into the final clearing prices. Under option 2, inequality (28) indicates that for a security constraint i, the summation of the shadow price of all events will not exceed the demand curve price $\Psi_{i,t}^{PED}$. Inequality (29) shows that the summation of post-STR event power balance shadow prices overall events will not exceed the demand curve price Ψ_t^{PB} .

III. NUMERICAL RESULTS

To validate the effectiveness and performance of proposed zonal and nodal post STR formulation, 289 consecutive 5-min real-time MISO test cases from one market day are used. MI-SO solves one of the largest and most complicated electricity market clearing problems in the world. MISO serves fifteen US states and one Canadian province. MISO's network model has over 45,000 buses and around 2,450 distinct commercial pricing nodes with 175GW generating capacity and around 125GW peak load. For each case of the 289 consecutive realtime MISO test cases, energy and ancillary service are cooptimized with the zonal STR model and nodal STR model in the real-time SCED. All results in this section were performed on 3.40 GHz CPU RAM 16 GB with AIMMS4.2 and CPLEX12.6 under Windows 7 Operating System. The simulations were performed on the prototype software that read case data stored in the flat files. The data were read by AIMMS using C++ based I/O library. A typical SCED problem has a scale of 10,000 rows and 10,000 columns. Note that computational time between the nodal model and zonal model does not have a noticeable difference since the nodal model does not complicate the mathematical model. The average solution for the zonal model is 23.4 seconds and the average solution for the nodal model is 23.7 seconds including the data reading time.

A. Zonal STR vs Nodal STR

Contingency analysis (CA) is performed to test the reserve deliverability of zonal and nodal STR models. CA evaluates flows after each online generator tripping followed by responses from cleared STR capacity. Lower violation value indicates better reserve deliverability. Fig.1 shows the histogram of average violation of contingency analysis. The zonal model tends to have more violations than the nodal model

especially for the intervals with the most congestion. From Fig. 2, the expected violation of each SCED period is presented for each period based on 289 study periods. For most of the periods, the nodal model has much less expected violation. The average expected violation of the zonal model is 1.91MW with a standard deviation of 3.13MW and the average expected violation of the nodal model is 1.67MW with a standard deviation of 2.98MW. Therefore, on average, the nodal model improves reserve deliverability by 12.6%. The total MWh violations are 45.84MWh for the zonal model and 40.08MWh for the nodal model. The results in Fig. 1 and Fig. 2 indicate that the nodal model improves the modeling accuracy and better formulate the post STR reserve deployment. Note the post deployment transmission constraints are applied only to constraints across the zones. Under the current tariff, reserve zone configuration is updated quarterly and can only be redefined under extreme events within a guarter. Nodal model can be effective for constraints within a zone and provide flexibility to address any post event transmission issues when needed. Nodal model is expected to have a much bigger benefit when constraints within a zone are considered. Currently, operators use manual disqualification to address those issues and it requires a significant amount of work to identify and remove operators' manual action in order to evaluate the benefit on constraints within a zone in production.

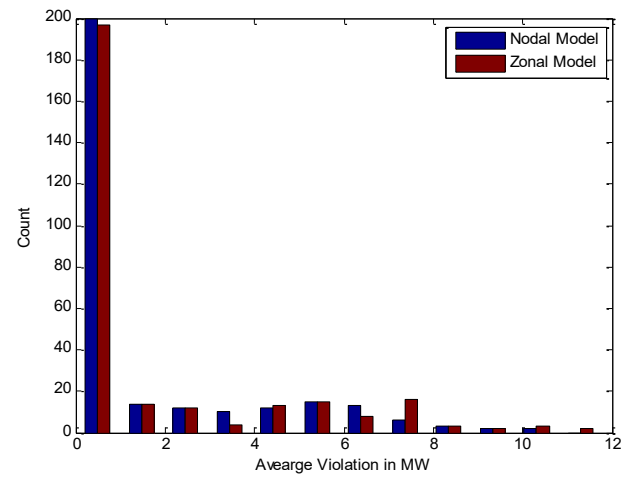


Fig.1 Histogram of Average Violation for Zonal and Nodal Models

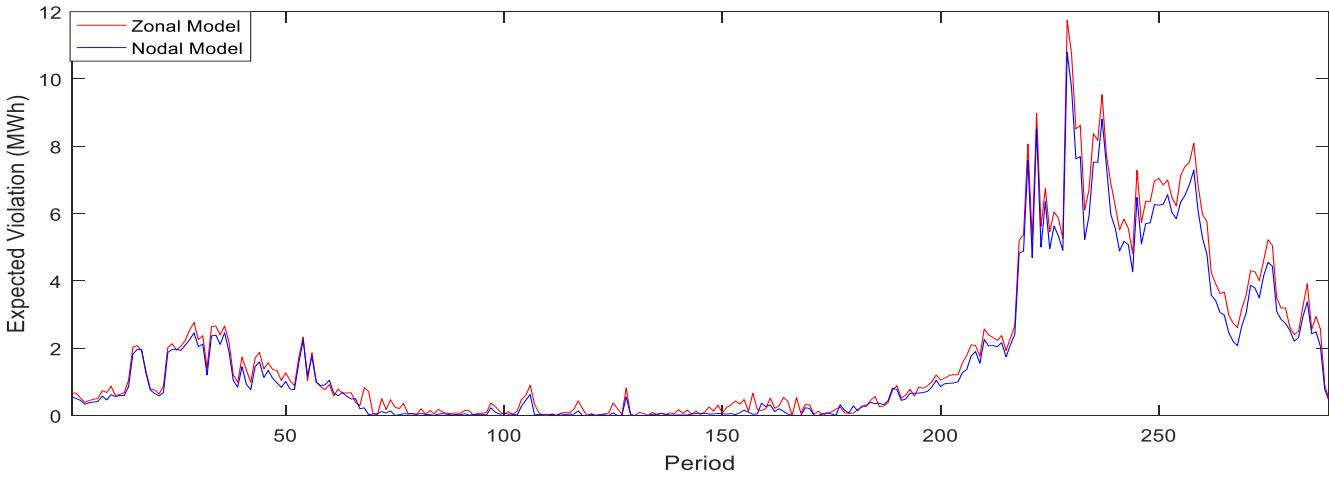


Fig. 2 Expected Violation of Each SCED period

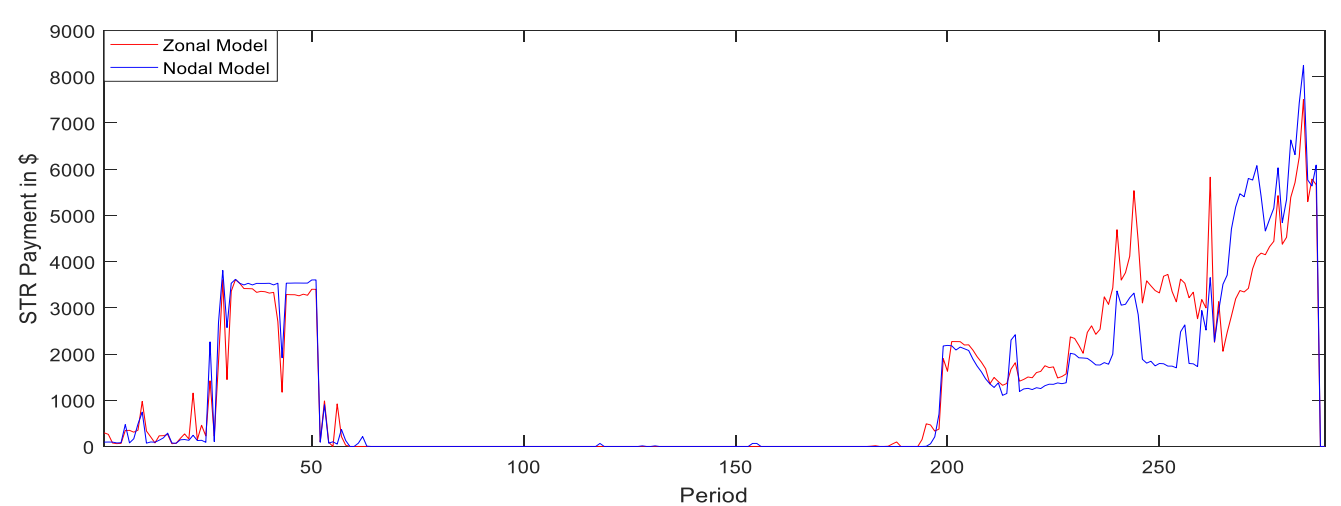


Fig. 3 STR Payment of Each SCED Period

Fig. 3 shows the STR payment of each SCED period. It can be easily observed that the STR payments are close to each other for most of the periods. Most of SCED periods have zero or near-zero STR payments because, for most of the periods,

STR post-event deliverability constraints are not binding. On average, STR payment of the zonal model has \$1,247 for each period and STR payment of nodal model has \$1,206 for each period. Note that the nodal model post-event deliverability

constraints are not necessarily tighter than the zonal model. The zonal model in periods 200-271 receives more STR payments than the nodal model since some cheap generating resources have higher post-event congestion relief in the nodal model than zonal model due to the zonal and nodal sensitivity differences. The zonal model needs to clear more zonal reserve for that zone to mitigate STR post-event deliverability constraint. For periods 271-289, the nodal model receives more STR payments than the zonal model. The nodal model needs to clear STR in specific locations, which are more expensive, to mitigate post-event congestion. This results in less expected violations in the nodal model.

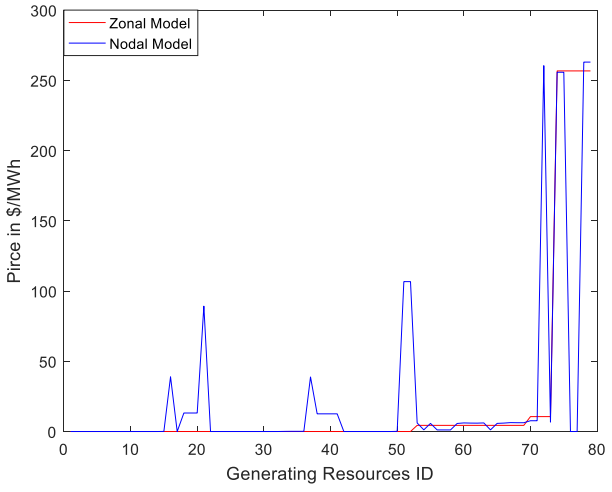


Fig. 4 STR prices for Zonal model and Nodal Model in Period 284

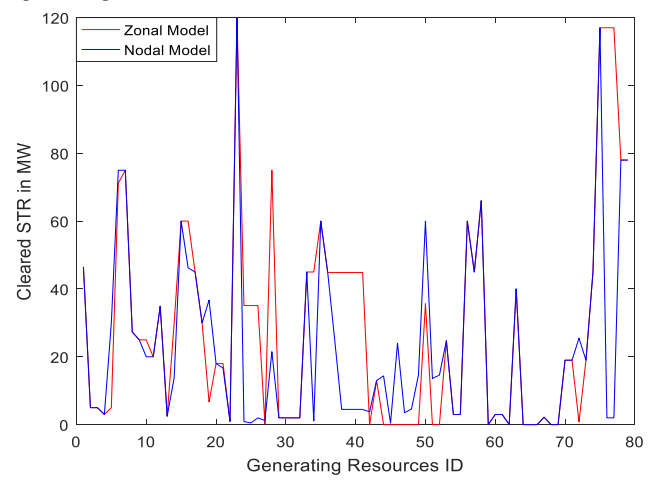


Fig. 5 Cleared STR MWs of Zonal Model and Nodal Model in Period 284

Period 284, which receives the highest STR payment for both the nodal model and zonal model, is selected to demonstrate STR price on a resource level. Fig. 4 presents the STR prices for the resources that clear STR in period 284. The STR prices of the zonal model are the same for resource in the same zone, for example, generating resources 74-79 are in the same reserve zone and share the same STR price \$257/MWh. The STR price of the nodal model is developed based on nodal STR deliverability. The positive congestion component in STR price indicates better deliverability and high STR price is usually associated with a higher value of congestion component. The STR price of the nodal model differs by resource nodal location and sends a better price signal.

Fig. 5 shows cleared MWs of STR by generating resources of the nodal model and zonal model. It is noteworthy that gen-

erating resources 76 and 77 clear 117MW each by zonal model while they clear only 2MW each by nodal. Generating resources 76 and 77 receive STR price at \$257/MWh from the zonal model and \$0/MWh from nodal mode. The zonal sensitivity of generating resources 76 and 77 on a binding security constraint is -0.23 while the actual nodal sensitivity of them on the binding security constraint is 0.13. The security constraint is binding in a positive direction and thus generating resources 76 and 77 do not help mitigate congestion on the binding constraints. Zonal model may clear the STR resources at these nodes due to the inaccuracy of aggregated zonal sensitivities, and the cleared STR will be undeliverable. Therefore, the nodal STR model is more effective to procure deliverable STR with better price signals.

B. Penalty Function Design

In the test cases, assume the demand curve prices for STR post-event power balance constraints and STR post-event deliverability constraints are set as \$500/MWh and \$300/MWh. Note that the demand curves should be deliberately chosen to reflect the true value of associated market product. There are eight reserve zones in MISO footprint and the largest generator tripping event is modeled for each zone. When the STR deliverability constraints bind for multiple STR events, Option 1 will accumulate associated shadow price while Option 2 will only consider the shadow price from the most severe event.

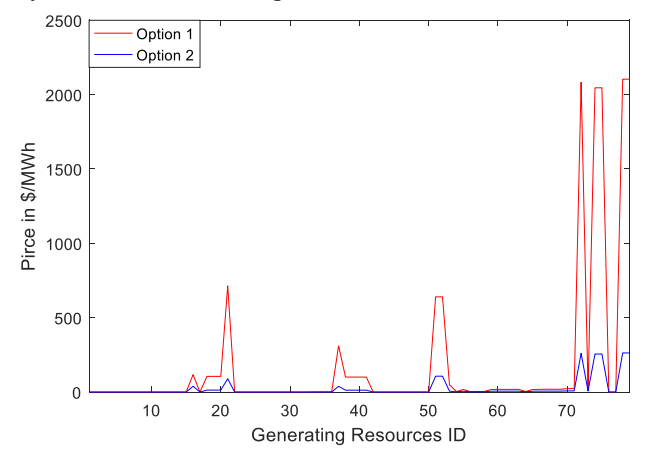


Fig. 6 STR prices of Option 1 and Option 2

Fig. 6 presents the STR prices with different demand curves and slack variables design options. It can be observed that for some of the units, the STR price of Option 1 could reach over \$2,000/MWh. Option 1 may overvalue STR postevent power balance constraints and STR post-event deliverability constraints. With eight events modeled, the theoretical highest congestion component for STR can be as high as \$2400/MWh. Option 2 caps the summated shadow prices of a security constraint overall events by \$300/MWh.

IV. CONCLUSION

This paper proposed a novel reserve requirements formulation, which incorporates event-based STR requirements. Two models, the zonal model and nodal model, are proposed to improve STR post-event deliverability. Reserve acquired based on the zonal approach does not model STR deployment with a resolution as accurate as the nodal model. Based on the numerical results, the nodal model of STR can improve the

reserve deliverability and lower expected post-event constraint violations. Lower expected post-event constraint violations could reduce or avoid out of market corrections.

The market impacts of the proposed zonal model and nodal model are also studied in this paper. The nodal model provides pricing signals on a nodal basis to better value the products provided by generating resources. Locational reserve price signal is supposed to attract investment of constructing flexible generating resources, such as energy storage and gas units. To further balance system efficiency and reliability, the proposed demand curve design can address the issue of overvaluing transmission assets for event-based security constraints.

V. APPENDIX

A. Existing MISO SCED Formulation

The existing SCED formulation in MISO [13] is described in this section. Note that the symbol following each type of constraint represents corresponding shadow prices.

$$\min_{p_{j,t},r_{j,t}^{x}} \sum_{j \in J} \left\{ C_{j,t}^{p} p_{j,t} + \sum_{x \in X} \left(O_{j,t}^{x} r_{j,t}^{x} \right) \right\}$$
(30)

Subject to:

Power balance equation (λ_t)

$$\sum_{j \in J} p_{j,t} + \sum_{n \in N} P_{n,t} = 0 \tag{31}$$

Transmission constraints $(\mu_{i,t})$

$$f_{i,t} = \sum_{j \in J} (p_{j,t} B_{i,n_{j,t}}) + \sum_{n \in N} (P_{n,t} B_{i,n,t}) \quad \forall i \in I$$
 (32)

$$f_{i,t} \le \overline{F}_{i,t} \quad \forall i \in I$$
 (33)

System-wide regulation reserve requirement (
$$\gamma_t^{MRR}$$
)
$$\sum_{k \in K} y_{k,t}^{REG} \ge R_{MKT,t}^{REG}$$
(34)

System-wide regulation/spinning reserve requirement (γ_{t}^{MRS})

$$\sum_{k \in K} (y_{k\,t}^{REG} + y_{k\,t}^{SPIN}) \ge R_{MKT\,t}^{REG} + R_{MKT\,t}^{SPIN} \tag{35}$$

System-wide operating reserve requirement (γ_t^{MOR})

$$\sum_{k \in K} (y_{k,t}^{REG} + y_{k,t}^{SPIN} + y_{k,t}^{SUPP}) \ge R_{MKT,t}^{REG} + R_{MKT,t}^{SPIN} + R_{MKT,t}^{SUPP}(36)$$

Zonal regulation reserve requirement $(\gamma_{k,t}^{ZRR})$

$$\sum_{j \in J^k} r_{j,t}^{REG} \ge y_{k,t}^{REG} \tag{37}$$

Zonal regulation/spinning reserve requirement ($\gamma_{k,t}^{ZRS}$)

$$\sum_{j \in J^k} (r_{jt}^{REG} + r_{jt}^{SPIN}) \ge y_{k,t}^{REG} + y_{k,t}^{SPIN}$$
(38)

Zonal operating reserve requirement (γ_t^{ZOR})

$$\sum_{i \in I^k} (r_{jt}^{REG} + r_{jt}^{SPIN} + r_{jt}^{SUPP}) \ge y_{k,t}^{REG} + y_{k,t}^{SPIN} + y_{k,t}^{SUPP}$$
 (39)

Post regulation reserve up deployment ($\mu_{i,t}^{REGUP}$)

$$f_{i,t} + \sum_{k \in K} (r_{k,t}^{REG} B_{i,k,t}^{REG}) - B_{i,LC,t} R_{MKT,t}^{REG} \le \overline{F}_{i,t}$$
 (40)

Post regulation reserve down deployment $(\mu_{i,t}^{REGDN})$

$$f_{i,t} - \sum_{k \in K} (r_{k,t}^{REG} B_{i,k,t}^{REG}) + B_{i,LC,t} R_{MKT,t}^{REG} \le \overline{F}_{i,t}$$

$$\tag{41}$$

Post CR zonal contingency event $(\mu_{i,\rho,t}^{CR})$

$$f_{i,t} - E_{e,t}^{CR} B_{i,k,t}^{TRIP} + D_{e,t}^{SPIN} \sum_{k \in K} (y_{k,t}^{SPIN} B_{i,k,t}^{SPIN}) + D_{e,t}^{SUPP} \sum_{k \in K} (y_{k,t}^{SUPP} B_{i,k,t}^{SUPP}) \le \overline{F}_{i,t}$$
(42)

Resource capacity constraints

$$p_{j,t} + r_{j,t}^{REG} + r_{j,t}^{SPIN} + r_{j,t}^{SUPP} \le U_{j,t} \overline{P}_{j,t}$$
 (43)

$$p_{j,t} - r_{j,t}^{REG} \ge U_{j,t} \underline{P}_{j,t} \tag{44}$$

Ramp constraints

$$-L_t V_{j,t}^{DOWN} \le p_{j,t} - P_{j,t-1} \le L_t V_{j,t}^{UP}$$
 (45)

$$0 \le r_{i,t}^{x} \le \overline{R}_{i,t}^{x} \tag{46}$$

Where
$$D_{e,t}^{SPIN} = \min \{1, \frac{E_{e,t}^{CR}}{R_{MKT}^{SPIN}}\}$$
 and $D_{e,t}^{SUPP} =$

$$\max \{0, \frac{E_{e,t}^{CR} - R_{MKT,t}^{SPIN}}{R_{MKT,t}^{SUPP}} \}.$$

The objective, (30), minimizes operating costs. Constraint (31) ensures total generation meets total demand. Constraint (32) is the linearized real power line flow equation. Constraint (33) imposes the transmission line's rating. In [13], SCED is enhanced by incorporating post zonal reserve deployment and modeling the largest contingency in each reserve zone for operating reserves, and the associated constraints are presented in constraints (33)-(42). Contingency reserves are modeled as proportionally deployed, which is consistent with MISO production deployment logic. The activation schemes of Post CR zonal contingency event constraint (42) reflect the MISO deployment process based on proportional deployment of spinning reserve followed by supplemental reserve. Constraints (43) and (44) presents minimum and maximum outputs. Constraint (43) indicates that regulation reserve does not share capacity with spinning and supplemental reserves. Constraints (45) and (46) are the ramp rate constraints for energy and reserves, respectively.

B. KKT Condition

The LMP can be expressed as a function of Lagrange multipliers based on the KKT condition.

 $LMP_{n,t}^{ZSTR}$ for the zonal model can be derived as below: $\partial \left(\sum_{i \in I} \left(C_{i,t}^{P} p_{i,t} + \sum_{x \in X} \left(O_{i,t}^{x} r_{i,t}^{x}\right)\right) + \lambda_{t} \left(\sum_{i \in I} p_{i,t} + \sum_{n \in N} P_{n,t}\right) + \lambda_{t} \left(\sum_{i \in I} p_{i,t} + \sum_{n \in N} P_{n,t}\right) + \lambda_{t} \left(\sum_{i \in I} p_{i,t} + \sum_{n \in N} P_{n,t}\right) + \lambda_{t} \left(\sum_{i \in I} p_{i,t} + \sum_{n \in N} P_{n,t}\right) + \lambda_{t} \left(\sum_{i \in I} p_{i,t} + \sum_{n \in N} P_{n,t}\right) + \lambda_{t} \left(\sum_{i \in I} p_{i,t} + \sum_{n \in N} P_{n,t}\right) + \lambda_{t} \left(\sum_{i \in I} p_{i,t} + \sum_{n \in N} P_{n,t}\right) + \lambda_{t} \left(\sum_{i \in I} p_{i,t} + \sum_{n \in N} P_{n,t}\right) + \lambda_{t} \left(\sum_{i \in I} p_{i,t} + \sum_{n \in N} P_{n,t}\right) + \lambda_{t} \left(\sum_{i \in I} p_{i,t} + \sum_{n \in N} P_{n,t}\right) + \lambda_{t} \left(\sum_{i \in I} p_{i,t} + \sum_{n \in N} P_{n,t}\right) + \lambda_{t} \left(\sum_{i \in I} p_{i,t} + \sum_{n \in N} P_{n,t}\right) + \lambda_{t} \left(\sum_{i \in I} p_{i,t} + \sum_{n \in N} P_{n,t}\right) + \lambda_{t} \left(\sum_{i \in I} p_{i,t} + \sum_{n \in N} P_{n,t}\right) + \lambda_{t} \left(\sum_{i \in I} p_{i,t} + \sum_{n \in N} P_{n,t}\right) + \lambda_{t} \left(\sum_{i \in I} p_{i,t} + \sum_{n \in N} P_{n,t}\right) + \lambda_{t} \left(\sum_{i \in I} p_{i,t} + \sum_{n \in N} P_{n,t}\right) + \lambda_{t} \left(\sum_{i \in I} p_{i,t} + \sum_{n \in N} P_{n,t}\right) + \lambda_{t} \left(\sum_{i \in I} p_{i,t} + \sum_{n \in N} P_{n,t}\right) + \lambda_{t} \left(\sum_{i \in I} p_{i,t} + \sum_{n \in N} P_{n,t}\right) + \lambda_{t} \left(\sum_{i \in I} p_{i,t} + \sum_{n \in N} P_{n,t}\right) + \lambda_{t} \left(\sum_{i \in I} p_{i,t} + \sum_{n \in N} P_{n,t}\right) + \lambda_{t} \left(\sum_{i \in I} p_{i,t} + \sum_{n \in N} P_{n,t}\right) + \lambda_{t} \left(\sum_{i \in I} p_{i,t} + \sum_{n \in N} P_{n,t}\right) + \lambda_{t} \left(\sum_{i \in I} p_{i,t} + \sum_{n \in N} P_{n,t}\right) + \lambda_{t} \left(\sum_{i \in I} p_{i,t} + \sum_{n \in N} P_{n,t}\right) + \lambda_{t} \left(\sum_{i \in I} p_{i,t} + \sum_{n \in N} P_{n,t}\right) + \lambda_{t} \left(\sum_{i \in I} p_{i,t} + \sum_{n \in N} P_{n,t}\right) + \lambda_{t} \left(\sum_{i \in I} p_{i,t} + \sum_{n \in N} P_{n,t}\right) + \lambda_{t} \left(\sum_{i \in I} p_{i,t} + \sum_{n \in N} P_{n,t}\right) + \lambda_{t} \left(\sum_{i \in I} p_{i,t} + \sum_{n \in N} P_{n,t}\right) + \lambda_{t} \left(\sum_{i \in I} p_{i,t} + \sum_{n \in N} P_{n,t}\right) + \lambda_{t} \left(\sum_{i \in I} p_{i,t} + \sum_{n \in N} P_{n,t}\right) + \lambda_{t} \left(\sum_{i \in I} p_{i,t} + \sum_{n \in N} P_{n,t}\right) + \lambda_{t} \left(\sum_{i \in I} p_{i,t} + \sum_{n \in N} P_{n,t}\right) + \lambda_{t} \left(\sum_{i \in I} p_{i,t} + \sum_{n \in N} P_{n,t}\right) + \lambda_{t} \left(\sum_{i \in N} P_{n,t}\right) + \lambda_{t} \left(\sum_{i \in I} p_{i,t} + \sum_{n \in N} P_{n,t}\right) + \lambda_{t} \left(\sum_{i \in I} p_{i,t} + \sum_{n \in N} P_{n,t}\right) + \lambda_{t} \left(\sum_{i \in I} p_{i,t} + \sum_{n \in$ $\sum_{i \in I} (\mu_{i,t} (f_{i,t} - \overline{F}_{i,t}) +$

$$\begin{split} & \sum_{i \in I^{REG}} \left(\mu_{i,t}^{REGUP} \left(f_{i,t} + \sum_{k \in K} (r_{k,t}^{REG} B_{i,k,t}^{REG}) - \overline{F}_{i,t} \right) \right. \\ & \left. + \right. \\ & \sum_{i \in I^{REG}} \left(\mu_{i,t}^{REGDN} \left(f_{i,t} - \sum_{k \in K} (r_{k,t}^{REG} B_{i,k,t}^{REG}) - \overline{F}_{i,t} \right) \right. \end{split}$$

$$\sum_{i \in I^{CR}} \sum_{e \in \mathcal{E}^{CR}} \frac{(\mu_{i,e,t}^{CR}(f_{i,t} + D_{e,t}^{SPIN} \sum_{k \in K} (y_{k,t}^{SPIN} B_{i,k,t}^{SPIN})}{+D_{e,t}^{SUPP} \sum_{k \in K} (y_{k,t}^{SUPP} B_{i,k,t}^{SUPP}) - \overline{F}_{i,t})}$$

$$+ \sum_{i \in I^{STR}} \sum_{e \in \mathcal{E}^{STR}} \mu_{i,e,t}^{ZSTR} (f_{i,t} + \sum_{k \in K} (q_{k,e,t}^{STR} B_{i,k,t}^{STR}) - \overline{F}_{i,t})$$

$$\frac{\sum_{i \in I} STR \sum_{e \in \mathcal{E}} STR \mu_{i,e,t}^{ZSTR} (f_{i,t} + \sum_{k \in K} (q_{k,e,t}^{STR} B_{i,k,t}^{STR}) - \overline{F}_{i,t})}{\partial P_{n,t}}$$

$$= \lambda_t + \sum_{i \in I} \mu_{i,t} B_{i,n,t} + \sum_{i \in I} REG (\mu_{i,t}^{REGUP} + \mu_{i,t}^{REGDN}) B_{i,n,t} + \sum_{i \in I} CR \sum_{e \in \mathcal{E}} CR \mu_{i,e,t}^{CR} B_{i,n,t} + \sum_{i \in I} STR \sum_{e \in \mathcal{E}} STR \mu_{i,e,t}^{ZSTR} B_{i,n,t}$$

$$(47)$$

Where
$$f_{i,t} = \sum_{j \in J} (p_{j,t} B_{i,n_j,t}) + \sum_{n \in N} (P_{n,t} B_{i,n,t})$$

 $LMP_{n,t}^{NSTR}$ for the nodal model can be derived as below:

 $0885-8950 \ (c)\ 2020\ IEEE.\ Personal\ use\ is\ permitted,\ but\ republication/redistribution\ requires\ IEEE\ permission.\ See\ http://www.ieee.org/publications_standards/publications/rights/index.html\ for\ more\ information.$ Authorized licensed use limited to: University of Prince Edward Island. Downloaded on September 09,2020 at 05:25:23 UTC from IEEE Xplore. Restrictions apply.

$$\partial \left(\sum_{j \in J} \left(C_{j,t}^{P} p_{j,t} + \sum_{x \in X} \left(O_{j,t}^{x} r_{j,t}^{x} \right) \right) + \lambda_{t} \left(\sum_{j \in J} p_{j,t} + \sum_{n \in N} P_{n,t} \right) + \\ \sum_{i \in I} \left(\mu_{i,t} \left(f_{i,t} - \overline{F}_{i,t} \right) + \\ \sum_{i \in I} REG \left(\mu_{i,t}^{REGUP} \left(f_{i,t} + \sum_{k \in K} \left(r_{k,t}^{REG} B_{i,k,t}^{REG} \right) - \overline{F}_{i,t} \right) \\ + \\ \sum_{i \in I} REG \left(\mu_{i,t}^{REGUP} \left(f_{i,t} - \sum_{k \in K} \left(r_{k,t}^{REG} B_{i,k,t}^{REG} \right) - \overline{F}_{i,t} \right) \\ + \\ \sum_{i \in I} REG \left(\mu_{i,t}^{REGDN} \left(f_{i,t} - \sum_{k \in K} \left(r_{k,t}^{REG} B_{i,k,t}^{REG} \right) - \overline{F}_{i,t} \right) \\ + \\ \sum_{i \in I} CR \sum_{e \in \mathcal{E}} CR \left(\mu_{i,t}^{REGDN} \left(f_{i,t} + \sum_{k \in K} \left(r_{k,t}^{REG} B_{i,k,t}^{REG} \right) - \overline{F}_{i,t} \right) \\ + \\ \sum_{i \in I} CR \sum_{e \in \mathcal{E}} CR \left(\mu_{i,t}^{REGDN} \left(f_{i,t} + \sum_{k \in K} \left(r_{k,t}^{REG} B_{i,k,t}^{REG} \right) - \overline{F}_{i,t} \right) \\ + \\ \sum_{i \in I} CR \sum_{e \in \mathcal{E}} CR \left(\mu_{i,t}^{REGDN} \left(f_{i,t} + \sum_{k \in K} \left(r_{k,t}^{REG} B_{i,k,t}^{REG} \right) - \overline{F}_{i,t} \right) \\ + \\ \sum_{i \in I} CR \sum_{e \in \mathcal{E}} CR \left(\mu_{i,t}^{REGDN} \left(f_{i,t} + \sum_{k \in K} \left(r_{k,t}^{REG} B_{i,k,t}^{REG} \right) - \overline{F}_{i,t} \right) \\ - \\ \sum_{i \in I} CR \sum_{e \in \mathcal{E}} CR \left(\mu_{i,e,t}^{REGDN} \left(f_{i,t} + \sum_{k \in K} \left(r_{k,t}^{REG} B_{i,k,t}^{REG} \right) - \overline{F}_{i,t} \right) \\ - \\ \sum_{i \in I} CR \sum_{e \in \mathcal{E}} CR \left(\mu_{i,e,t}^{REGDN} \left(f_{i,t} + \sum_{k \in K} \left(r_{k,t}^{REG} B_{i,k,t}^{REG} \right) - \overline{F}_{i,t} \right) \\ - \\ \sum_{i \in I} CR \sum_{e \in \mathcal{E}} CR \left(\mu_{i,e,t}^{REGDN} \right) \left(f_{i,t} + \sum_{k \in K} \left(r_{k,t}^{REG} B_{i,k,t}^{REGDN} \right) - \overline{F}_{i,t} \right) \\ - \\ \sum_{i \in I} CR \sum_{e \in \mathcal{E}} CR \left(\mu_{i,e,t}^{REG} B_{i,n,t} + \sum_{i \in I} CR B_{i,e,t}^{REGDN} \right) B_{i,n,t} + \\ \sum_{i \in I} CR \sum_{e \in \mathcal{E}} CR \left(\mu_{i,e,t}^{REG} B_{i,n,t} + \sum_{i \in I} CR B_{i,e,t}^{REGDN} \right) B_{i,n,t} + \\ \sum_{i \in I} CR \sum_{e \in \mathcal{E}} CR \left(\mu_{i,e,t}^{REG} B_{i,n,t} + \sum_{i \in I} CR B_{i,e,t}^{REGDN} \right) B_{i,e,t} + \\ \sum_{i \in I} CR \sum_{e \in \mathcal{E}} CR \left(\mu_{i,e,t}^{REG} B_{i,n,t} + \sum_{i \in I} CR B_{i,e,t}^{REGDN} B_{i,e,t}^{REGDN} \right) B_{i,e,t} + \\ \sum_{i \in I} CR \sum_{e \in \mathcal{E}} CR \left(\mu_{i,e,t}^{REG} B_{i,e,t} + \sum_{i \in I} CR B_{i,e,t}^{REGDN} B_{i,e,t}^{REGDN} \right) B_{i,e,t} + \\ \sum_{i \in I} CR \sum_{e \in$$

VI. REFERENCES

Where $f_{i,t} = \sum_{i \in I} (p_{i,t} B_{i,n_i,t}) + \sum_{n \in N} (P_{n,t} B_{i,n,t})$

- [1] J. M. Arroyo and F. D. Galiana, "Energy and reserve pricing in security and network-constrained electricity markets," IEEE Trans. Pow er Syst., vol. 20, no. 2, pp.634-643, 2004.
- T. Zheng and E. Litvinov, "Contingency-based zonal reserve modeling and pricing in a co-optimized energy and reserve market," IEEE Trans. Power Syst., vol. 23, no. 2, pp. 277-286, May 2008.
- F. Galiana, F. Bouffard, J. M. Arroyo, and J. F. Restrepo, "Scheduling and pricing of coupled energy and primary, secondary, and tertiary reserves," Proc. IEEE, vol. 93, no. 11, pp. 1970-1983, Nov. 2005.
- SANDIA Report, "Project report: a survey of operating reserve markets in U.S. ISO/RTO-managed electric energy regions", Sep. 2012. [Online]. Available: http://prod.sandia.gov/techlib/accesscontrol.cgi/2012/121000.pdf
- CAISO, "Intra-zonal congestion," CAISO Dept. of Market Monitoring, 2007. Tech. Report., Apr. [Online]. Available: https://www.caiso.com/Documents/Chapter6 Intra-ZonalCongestion.pdf
- CAISO, "2018 annual report on market issues & performance," May. [6] [Online]. Available: http://www.caiso.com/Documents/2018AnnualReportonMarketIssuesan dPerformance.pdf
- ERCOT. "ERCOT Protocols. Available: [Online]. http://www.ercot.com/content/mktrules/protocols/library/2010/02/Febru ary 1, 2010 Protocols.pdf
- ERCOT, "Report on existing and potential electric system constraints and needs," ERCOT System Planning and Transmission Services. Available: http://www.ercot.com/content/news/presentations/2013/2012%20Constr aints%20and%20Needs%20Report.pdf
- MISO, "Tariff," Midcontinent Independent System Operator, 2012. https://www.misoenergy.org/ layouts/MISO/ECM/Download.aspx?ID= 169142
- [10] F. Wang and K. W. Hedman, "Reserve zone determination based on statistical clustering method," in Proc. North American Power Svmp., 2012.
- [11] F. Wang and K. W. Hedman, "Dynamic reserve zones for day-ahead unit commitment with renewable resources," IEEE Trans. Power Syst., vol. 30, no. 2, pp. 612-620, Mar. 2015.
- [12] J. Lyon, F. Wang, K. W. Hedman, and M. Zhang, "Market implications and pricing of dynamic reserve policies for systems with renewables", IEEE Trans. Power Syst., vol. 30, no. 3, pp. 1593-1602, May 2015.
- Y. Chen, P. Gribik, and J. Gardner, "Incorporating post zonal reserve deployment transmission constraints into energy and ancillary services co-optimization," IEEE Trans. Power Syst., vol. 29, no. 2, pp. 537-549, Mar. 2014.
- [14] L. Morelli, "Reserve zone & synchronized reserve market proposal overview" [Online]. Available: https://www.pjm.com/-/media/committees-groups/task-forces/epfstf/20180418/20180418-item-06-epfstf-reserve-zone-synchronized-reserve-market-proposaloverview.ashx

- under correlated nodal demand uncertainty: An adjustable robust optimization approach," International Journal of Electrical Power& Energy Systems, vol.72, pp. 91-98, Nov. 2015.
- [16] H. Ye and Z. Li, "Deliverable robust ramping products in real-time Markets," IEEE Trans. Power Syst., vol. 33, no. 1, pp. 5-18, Jan. 2018.
- [17] Q. Zhao, P. Wang, L. Goel, and Y. Ding, "Impacts of Contingency Reserve on Nodal Price and Nodal Reliability Risk in Deregulated Power Systems," IEEE Trans. Power Syst., vol. 28, no. 3, pp. 2497-2506, Aug. 2013.
- [18] P. Akbary, et. al., "Extracting appropriate nodal marginal prices for all types of committed reserve," Computational Economics, 2019.
- A. Papavasiliou, S. S. Oren, and R. P. O'Neill, "Reserve requirements for wind power integration: a scenario-based stochastic programming framework," IEEE Trans. Power Syst., vol. 26, no. 4, pp. 2197-2206, Nov. 2011.
- [20] K. W. Hedman, M. C. Ferris, R. P. O'Neill, E. B. Fisher, and S. S. Oren, "Co-optimization of generation unit commitment and transmission switching with N-1 reliability," IEEE Trans. Power Syst., vol. 25, no. 2, pp. 1052-1063, May 2010.
- [21] F. Bouffard and F. D. Galiana, "Stochastic security for operations planning with significant power generation," IEEE Trans. Power Syst., vol. 23, no. 2, pp. 306-316, May 2008.
- F. Bouffard and F. D. Galiana, A. J. Conejo, "Market-clearing with stochastic security - part I: formulation," IEEE Trans. Power Syst., vol. 20, no. 4, pp. 1818–1826, Nov 2005.
- [23] J. Wang, M. Shahidehpour, and Z. Li, "Contingency-constrained reserve requirements in joint energy and ancillary services auction", IEEE Trans. Power Syst., vol. 24, no. 3, pp. 1457-1468, Aug. 2009.
- Y. Chen, A. Casto, F. Wang, Q. Wang, X. Wang, and J. Wan, "Improving large scale day-ahead security constrained unit commitment performance," IEEE Trans. Power Syst., vol. 31, no. 6, pp. 4732-4743, Nov. 2016.
- Y. Chen, F. Wang, Y. Ma, and Y. Yao, "A distributed framework for solving and benchmarking security constrained unit commitment with warm start," IEEE Trans. Power Syst., vol. 65, no. 1, pp. 711-720, Jan. 2020.
- [26] J. Dupacová, N. Gröwe-Kuska, and W. Römisch, "Scenario reduction in stochastic programming: An approach using probability metrics," Math. Program, Series A, vol. 3, pp. 493-511, 2003.
- N. Gröwe-Kuska, H. Heitsch, and W. Römisch, "Scenario reduction and scenario tree construction for power management problems," in Proc. IEEE Power Tech Conf., Bologna, Italy, vol. 3, pp. 23-26, Jun. 2003.
- [28] F. C. Schweppe, M. C. Caramanis, R. D. Tabors, and R. E. Bohn, Spot Pricing of Electricity. Norwell, MA, USA: Kluwer, 1988.
- [29] W. Hogan and S. Pope, "PJM reserve markets: operating reserve demand curve enhancements", Mar. 2019. [Online]. Available: https://scholar.harvard.edu/whogan/files/hogan pope pim report 03211 9.pdf
- [30] MISO, "FERC Electric Tariff: Schedule 28A demand curves for transconstraints" Jul. 2019 mission [Online]. Available: https://cdn.misoenergy.org/Schedule%2028-A109699.pdf

Fengyu Wang (M'15) received the B.E. degree in electrical engineering from the Dalian University of Technology, China, and the M.S. degree in electrical and computer engineering from Boston University, Boston, MA, USA, in 2008 and 2010, respectively. He received the Ph.D. degree in electrical engineering from Arizona State University, Tempe, AZ, USA, in 2015. Currently, he is an assistant professor in Klipsch School of Electrical and Computer Engineering at New Mexico State University, Las Cruces NM, USA. Previously, he was a senior R&D Market Engineer with the Midcontinent Independent System Operator. His research interests include power system economics, operations, and planning.

Yonghong Chen (SM'12) received the B.S. degree from Southeast University, Nanjing, China, the M.S. degree from Nanjing Automation Research Institute, China, and the Ph.D. degree from Washington State University, Pullman, WA, USA, all in electrical engineering. She also received the M.B.A. degree from Indiana University, Kelly School of Business, Indianapolis, IN, USA. She is currently a Consulting Advisor with the Midcontinent Independent System Operator, Inc. In this role, she focuses on research and development to address challenges facing market design and market clearing systems. Before joining MISO in 2002, she worked with GridSouth Transco LLC and Nanjing Automation Research Institute.